Scattering of long waves by freely oscillating submerged plates

Chen, Yongbo; Hayatdavoodi, Masoud; Zhao, Binbin ; Ertekin, R. Cengiz

Published in:
Journal of Offshore Mechanics and Arctic Engineering

Publication date:
2024

Scattering of long waves by freely oscillating submerged plates

Yongbo Chen
College of Shipbuilding Engineering
Harbin Engineering University
Harbin, China

Masoud Hayatdavoodi *
Civil Engineering Department
University of Dundee
Dundee, DD1 4HN, UK
& College of Shipbuilding Engineering
Harbin Engineering University
Harbin, China

Binbin Zhao
College of Shipbuilding Engineering
Harbin Engineering University
Harbin, China

R. Cengiz Ertekin †
Ocean and Resources Engineering Department
SOEST, University of Hawaii at Manoa
2540 Dole St., Holmes 402, Honolulu, HI 96822
& College of Shipbuilding Engineering
Harbin Engineering University
Harbin, China

ABSTRACT

We consider a horizontal, submerged plate in shallow water that is allowed to oscillate in the vertical direction due to the wave loads. The plate is attached to a linear spring and damper to control the oscillations. The focus of the study is on the transformation of the wave field by the submerged oscillating plate. To estimate energy scattering, wave reflection and transmission coefficients are determined from four wave gauges; two placed upwave and two placed downwave of the oscillating plate. The flow is governed by the nonlinear Level I Green-Naghdi (GN) equations, coupled with the equations of the

*Address all correspondence to M. Hayatdavoodi (mhayatdavoodi@dundee.ac.uk).
†Fellow, ASME

vertical oscillations of the plate. Time series of water surface elevation recorded at gauges upwave and downwave of the plate obtained by the GN model are compared with the available laboratory experiments and other data, and very good agreement is observed. Wave reflection and transmission coefficients are then determined for a range of involved parameters, including wave conditions (wavelength and wave height), initial submergence depth of the plate, plate length, and the spring-damper system attached to the plate. It is found that a submerged oscillating plate can have a remarkable effect on the wave field, and that nonlinearity plays an important role in this wave-structure interaction problem. Discussion is provided on how the wave reflection and transmission coefficients vary with the wave conditions, plate characteristics, initial submergence depth and spring-damper system properties.

Keywords: *Submerged oscillating plates, GN equations, shallow water waves, wave reflection and transmission*

1 INTRODUCTION

Submerged oscillating plates are used in floating structures to reduce heave oscillations, in energy devices to convert the wave energy into electricity, and in breakwaters to mitigate extreme wave impact on nearshore and coastal structures. Wave scattering characteristics by submerged fixed plates have been investigated by many researchers, see e.g. [1], [2], [3], [4], [5] and [6]. Compared to submerged fixed plates, oscillating horizontal plates are more efficient to scatter waves, as illustrated by [7], [8] and [9]. Submerged horizontal plates are also applied as submerged wave energy devices and they modify the wave field, see e.g. [10] and [11] for the effect of submerged wave energy devices on the wave field. Wave deformation by submerged horizontal plates used in wave energy devices are investigated by e.g. [12] and [13], and by e.g. [14] and [15] for an array of plates.

Submerged horizontal plates experience oscillatory loads due to wave propagation. The horizontal plate, if designed appropriately for the purpose, can oscillate in the vertical direction due to the vertical wave-induced force. At the same time, oscillations of the plate also alter the wave field, i.e. wave loads result in plate oscillations, and the plate oscillations results in formation of waves and wave scattering. Hence, this is a fluid-structure-fluid problem, understanding of which requires knowledge about the fluid domain, fluid-induced oscillations of the plate, and the effect of the plate on the fluid domain, and the coupling between these. Wave-induced oscillations of the plate are affected by various parameters, including wave conditions, initial submergence depths of the plate, and the attached spring-damper system which is used to control plate's oscillations.

Many studies are performed to understand transformation of waves propagating over a submerged fixed plate, see e.g. [4], [16] and [17]. By comparing surface elevation time series upwave and downwave of the plate, [18] illustrated that waves scattered by an oscillating plate are different compared to a fixed plate case. However, investigations of wave scattering by a submerged oscillating plate are very limited.

Wave scattering by oscillating plates were studied numerically by [7], [8] and [9]. In the work of [7], a numerical wave tank was established by use of the linear potential theory, to investigate how waves are scattered by a submerged oscillating horizontal plate, and wave reflection and transmission coefficients are calculated to determine the wave scattering. In that study, the plate was attached to a spring and critical spring stiffness values were determined to reduce the wave transmission coefficients to near zero. By use of the smoothed particle hydrodynamics method, wave scattering by an oscillating plate for various initial submergence depths was investigated by [8]. On the other hand, by use of a computational fluid dynamics method, [9] considered the effect of wavelength on wave scattering by oscillating plates. These studies, however, are confined to interaction of short waves with oscillating plates in deep to intermediate water conditions subject to very limited wave-plate cases.

Submerged oscillating horizontal plates, used for mitigation of large waves and for wave energy production applications, are generally placed in shallow waters. Wave transformation in shallow water over an irregular seafloor or by an object requires a proper understanding of the importance of nonlinearity, i.e. the ratio of wave height to water depth, and dispersion, the ratio of water depth to wavelength. The nonlinearity plays an important role when wave propagates over a freely oscillating submerged plate due to the sudden change of the water depth upwave and above the plate. Dispersion, on the other hand, causes the formation of higher oscillatory components as the wave passes over the plate towards the downwave region. Thus, the knowledge of proper understanding of wave nonlinearity and dispersion is essential in the solution of the problem of wave scattering by submerged oscillating plates.

In this study, we use a nonlinear, dispersive approach to study wave scattering by a submerged, oscillating horizontal plate, namely through the Level I Green-Naghdi (GN) equations. We follow a similar approach recently proposed by [19] to study this problem. The wave scattering is investigated by defining wave reflection and transmission coefficients.

We consider a plate that is initially at rest. The plate undergoes oscillations due to wave propagation. The plate is allowed to oscillate only in the vertical direction by use of guide rails and its oscillations are controlled by a linear spring and damper. A wide range of parameters are considered, including wave condition, plate length, initial submergence depth of the plate, spring stiffness and damping coefficient, and their effects on the wave reflection and transmission is studied.

The Level I GN theory is introduced first, followed by the equation of motion of the plate. Qualitative results of wave scattering by a submerged oscillating and fixed plate are first shown for a solitary wave. Results of surface elevation time series of periodic waves are then compared with the available data. This is followed by discussion on cnoidal wave scattering by an oscillating submerged horizontal plate. Then variations of wave reflection and transmission coefficients with different variables are presented and discussed, where contributions of higher-order harmonics are also investigated. Results of the oscillating plate problem are then compared to a fixed, horizontal plate problem. The concluding remarks section is followed to close the paper.

2 THE LEVEL I GN THEORY

The wave deformation by a submerged oscillating plate is studied here by developing a model based on the Level I GN equations. A right-handed Cartesian coordinate system is used in two dimensions, where x_1 points in the wave propagation direction and x_2 points up, against the gravity. The origin of the coordinate system is located on the still-water level (SWL). The fluid domain is bounded by top and bottom deformable curves, and the flow is assumed to be incompressible and inviscid.

The Green-Naghdi equations are a set of nonlinear, partial differential equations, introduced originally by [20] and [21], also to determine nonlinear wave motions. The GN equations satisfy the nonlinear boundary conditions and conservation of mass exactly, and postulate the conservation of momentum in an integrated form. There is no limitation for the irrotationality of the flow, i.e., the flow can be rotational, see [20]. The only assumption made about the fluid kinematics in the GN equations is the distribution of the vertical velocity over the fluid column, which determines the levels of the GN equations, see [21]. In the Level I GN model used in this study, the vertical velocity varies linearly within the water column and thus the horizontal velocity is invariant in the vertical direction. The Level I GN model is best applied to propagation of long waves in shallow water, see e.g. [4], [19] and [22]. For higher level GN equations, the vertical velocity field is prescribed in terms of high-order functions, see e.g. [23], [24] and [25]. Also, see [26] for refraction and diffraction of waves in shallow water due to uneven seafloor by the Level I GN equations.

The Level I GN equations are expressed by the conservations of mass and momentum statements as (see [27])

$$\eta_{,t} + \{(h+\eta-\alpha)u_1\}_{,x_1} = \alpha_{,t}\,, \tag{1}$$

$$\dot{u}_1 + g\eta_{,x_1} + \frac{\hat{p}_{,x_1}}{\rho} = -\frac{1}{6}\{[2\eta+\alpha]_{,x_1}\ddot{\alpha} + [4\eta-\alpha]_{,x_1}\ddot{\eta} + (h+\eta-\alpha)[\ddot{\alpha}+2\ddot{\eta}]_{,x_1}\}\,, \tag{2}$$

where u_1 and u_2 are the fluid particle velocities in the x_1 and x_2 directions, respectively, $\hat{p}$ is the pressure on the top surface of the fluid domain, α is the deformation of the bottom surface, η is the surface elevation, measured from the SWL, ρ is the fluid density and g is the gravitational acceleration. Subscripts after comma indicate differentiation with respect to the corresponding variables. $\dot{\theta}$ and $\ddot{\theta}$ are the first and second total or material derivatives of the arbitrary variable $\theta(x_1,t)$, respectively.

Following the approach proposed by [28] for wave propagation over a fixed, horizontal plate in studying wave interaction with a submerged oscillating plate, the fluid domain is divided into four regions shown in Fig. 1: (i) RI, $x_1 < X_L$, the upwave region from the leading edge of the plate, (ii) RII, $X_L \leq x_1 \leq X_T$, the region above the oscillating plate, (iii) RIII, $X_L \leq x_1 \leq X_T$, the region below the plate, and (iv) RIV, $x_1 > X_T$, the downwave region from the trailing edge of the plate. Appropriate governing equations and boundary conditions are applied to each region.

The schematic of the numerical wave tank of wave interaction with a submerged, oscillating horizontal plate is shown in Fig. 1. A wave-maker of capability of generating solitary and cnoidal waves of the GN theory, see e.g. [29] and [30], and a wave absorber by use of Sommerfeld's condition, see [31], are used on the left and right boundaries of the domain, respectively.

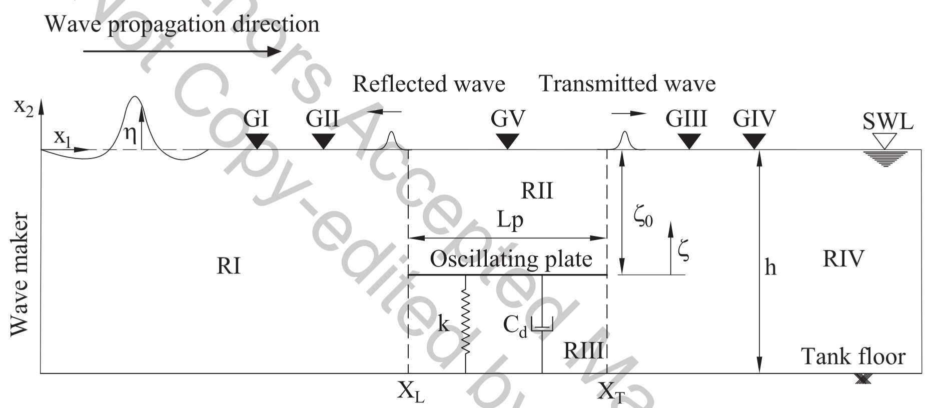

Fig. 1: Schematic of the numerical wave tank of wave interaction with a fully submerged horizontal oscillating plate. The length of the plate is L_P.

In Regions RI and RIV, the seafloor is flat and stationary, i.e. $\alpha(x_1,t) = 0$. The top boundary of the domain is free, i.e. $\eta = \eta(x_1,t)$, and it is exposed to the atmosphere, i.e. the top pressure is equal to the atmospheric pressure, taken as $\hat{p}(x_1,t) = 0$. Substituting $\alpha = \alpha_{,t} = \alpha_{,x_1} = 0$, $\hat{p} = 0$ and the constant water depth, $h = h_I$, into Eqs. (1) and (2), the resulting equations for regions RI and RIV are given as

$$\eta_{,t} + \{(h_I + \eta)u_1\}_{,x_1} = 0\,, \tag{3}$$

$$\dot{u}_1 + g\eta_{,x_1} = -\frac{1}{3}\{2\eta_{,x_1}\ddot{\eta} + (h_I + \eta)\ddot{\eta}_{,x_1}\}\,. \tag{4}$$

The unknowns in RI and RIV are the free surface elevation, η, and the horizontal velocity, u_1.

In Region RII above the oscillating plate, $\eta = \eta(x_1,t)$, and $\hat{p}(x_1,t) = 0$, similar to that in Regions RI and RIV. The bottom surface of Region RII is the oscillating plate. In this study, we assume that the plate is flat and rigid, and its oscillations are only allowed in the vertical direction, and that the water depth in RII is fixed at $h = h_{II} = \zeta_0$, also known as the initial submergence depth. Therefore, the vertical elevation of the plate in RII is given as $\alpha(x_1,t) = \alpha(t) = \zeta(t)$, where ζ is the instantaneous position of the plate measured from ζ_0. Substituting these conditions into Eqs. (1) and (2) gives the governing equations of wave propagation over a vertically oscillating floor as

$$\eta_{,t} + [(\zeta_0 + \eta - \zeta)u_1]_{,x_1} = \zeta_{,t}\,, \tag{5}$$

$$\dot{u}_1 + g\eta_{,x_1} = -\frac{1}{3}\{(\ddot{\zeta} + 2\ddot{\eta})\eta_{,x_1} + (\zeta_0 + \eta - \zeta)\ddot{\eta}_{,x_1}\}\,. \tag{6}$$

The unknowns in Region RII are η, u_1 and ζ. That is, in RII, the number of unknowns is one more than the number of the equations.

Region RIII consists of a horizontal, oscillating plate on its top, and a flat, stationary seafloor on the bottom, i.e. $\eta(x_1,t) = \eta(t)$ and $\alpha(x_1,t) = 0$ in RIII. The plate is assumed to be thin and thus the water depth in this region is $h = h_{III} = h_I - \zeta_0$. Substituting these conditions into Eqs. (1) and (2) gives

$$\eta_{,t} + (h_I - \zeta_0 + \eta)u_{1,x_1} = 0\,, \tag{7}$$

$$\dot{u}_1 + \frac{\hat{p}_{,x_1}}{\rho} = 0\,, \tag{8}$$

in which the unknowns are η, u_1, and $\hat{p}$, i.e. pressure under the plate. Similar to RII, the number of equations (2) in RIII is one less than the number of unknowns (3). Thus two more equations are required to close the system of equations in Regions RII and RIII.

We assume that the fluid is attached to the plate without any gaps at all times, i.e., $\eta_{III}(t) = \alpha_{II}(t) = \zeta(t)$, where subscripts II and III refer to the variables in the respective regions. As shown in Fig. 1, ζ is measured from the plate's initial submergence depth, ζ_0. This relation closes the system of equations in RIII. Substituting $\eta(x_1,t) = \zeta(t)$ into Eq. (7), and integrating with respect to x_1 gives

$$u_1 = C_1 x_1 + C_2(t), \tag{9}$$

where C_1 is at most a function of time only (independent of x_1), given as

$$C_1(t) = -\frac{\zeta_{,t}}{h_I - \zeta_0 + \zeta}\,, \tag{10}$$

and C_2 is the integration constant of time at most. Equation (9) illustrates that the horizontal velocity in RIII varies linearly in the x_1 direction. It is not physical to directly apply Eq. (9) for a very long plate as for $x_1 \to \infty$,we would have $u_1(\infty,t) \to \infty$. Therefore from Eq. (9), we assume that u_1 in RIII varies linearly between two ends of the plate i.e. its value is always bounded between the velocities at the leading and trailing edges for any plate length.

The momentum equation in RIII, Eq. (8), can be expanded as

$$u_{1,t} + u_1 u_{1,x_1} + \frac{\hat{p}_{,x_1}}{\rho} = 0\,. \tag{11}$$

Substituting Eq. (9) into Eq. (11), and integrating with respect to x_1 gives

$$\hat{p} = \frac{\rho}{2}\left(C_1^2 + C_{1,t}\right) x_1^2 + C_3(t), \tag{12}$$

where $C_3 = C_3(t)$ is the integration constant of time at most. That is, the top pressure in RIII i.e. pressure under the plate, varies parabolicly across the length of the plate.

Appropriate jump and matching conditions are enforced at the domain discontinuity curves, where the regions meet (the leading and trailing edges of the plate) to satisfy the physics of the problem, and demanded by the theory, see [32]. In this study, the matching and jump conditions at discrete surfaces includes: (i) the continuity of the surface elevation, and (ii) the Kutta condition, i.e. at the edges of the plate, the pressure above the plate is equal to that below the plate. See [19] for more details about the jump and matching conditions used in this study.

In the problem of wave interaction with a submerged oscillating plate, we assume that the plate is rigid and flat at all times. The vertical oscillation of the plate is controlled by a linear spring and damper. The plate oscillations are restricted to the vertical direction by use of guide rails, and hence its acceleration is described by $\zeta_{,tt}$. The wave-induced oscillations of the plate are therefore given by Newton's second law as

$$\Sigma F = m\zeta_{,tt}\,, \tag{13}$$

where m is the mass of the plate, and $\Sigma F = F_{x_2} + F_f + F_k + F_{PT}$ is the sum of the external loads on the plate, including (i) the vertical wave force, $F_{x_2}(t)$, (ii) the friction force between the plate and the guide rails, $F_f(t) = -\left(\frac{|\zeta_{,t}|}{\zeta_{,t}}\right)\mu F_{x_1}$, where $F_{x_1}(t)$ is the horizontal wave force on the plate and $\zeta_{,t}$ specifies the plate velocity, (iii) the spring force, $F_k(t) = -k(\zeta - \zeta_0)$, where k is the linear spring constant stiffness, and (iv) the damping force, $F_{PT}(t) = -C_d\zeta_{,t}$, where C_d is the damping coefficient. The plate is initially located at the equilibrium position ($x_2 = -\zeta_0$) where the weight of the plate, buoyancy and the spring forces are balanced. See [33] for discussion on nonlinear horizontal and vertical wave forces on the submerged plate. By introducing Eq. (13), we now obtain one additional equation for $\zeta(t)$, and the system of equations in Regions II and III are closed.

The entire system of equations are discretized by use of the finite-difference method. The fluid domain is discretized into a set of mesh points and all continuous variables are approximated by the discrete values at the mesh nodes. Spatial derivatives are approximated by use of the second-order central difference method. The second-order modified Euler method is applied for time-marching, and the Gaussian Elimination method is used to solve the systems of equations. At each time step, as the external forces are known, the plate oscillation is determined by use of the fourth-order Runge-Kutta method. See [19] and [31] for more details on the numerical solutions used in this model.

3 WAVE REFLECTION AND TRANSMISSION COEFFICIENTS

In this study, wave scattering by oscillating plates is determined by the wave reflection and transmission coefficients. To calculate the reflection and transmission coefficients, the four-gauge method of [34] is applied. In this approach Gauges GI and GII are placed upwave from the leading edge of the plate, and Gauges GIII and GIV are placed downwave from the trailing edge of the plate, shown in Fig. 1. This method has been used successfully by [4], [35] and [36] for problems involving nonlinear wave interaction with structures by the Level I GN equations.

The surface elevation at a given location (gauge) is split into a series of linear waves of different amplitude, frequency and phase by use of the Fourier Transform method. The reflected and transmitted wave amplitudes of the n^{th} order harmonic, $A_R^{(n)}$ and $A_T^{(n)}$, are decomposed from the surface elevations upwave and downwave, respectively. To better assess the nonlinear effects, the first three harmonic amplitudes ($n = 1,2$ and 3) are used to calculate wave reflection, C_R and transmission coefficients, C_T, given as

$$C_R^{(n)} = \frac{A_R^{(n)}}{A_I}, \quad C_T^{(n)} = \frac{A_T^{(n)}}{A_I}, \tag{14}$$

where A_I is the incident wave amplitude, and superscript (n) refers to n^{th} order harmonic of the Fourier Transform.

4 RESULTS AND DISCUSSION

Results of the GN model discussed in the previous section for scattering of long waves with a submerged plate is presented in this section. Results are given in these sub-sections, namely (i) solitary wave scattering, where we discuss the effect of submerged oscillating and fixed plate on wave scattering, (ii) comparisons of the results with available data, and (iii) scattering of cnoidal waves, where we discuss how various parameters affect the wave scattering.

In this paper, all variables are made dimensionless by use of ρ, g and h, such that

$$\begin{aligned} &x_1' = \frac{x_1}{h}, \quad \eta' = \frac{\eta}{h}, \quad \lambda' = \frac{\lambda}{h}, \quad H' = \frac{H}{h}, \quad L_P' = \frac{L_P}{h}, \quad \zeta_0' = \frac{\zeta_0}{h}, \\ &t' = t\sqrt{\frac{g}{h}}, \quad m' = \frac{m}{\rho h^2 B}, \quad k' = \frac{k}{\rho g h B}, \quad C_d' = \frac{C_d}{\rho\sqrt{gh}Bh}, \end{aligned} \tag{15}$$

where λ is wavelength, H is wave height, and B is the plate width (into the page). Superscript $(')$ is removed hereafter from all variables for simplicity.

4.1 Solitary Wave Scattering

In this part, solitary wave deformation by an oscillating plate is investigated. Results are presented in the form of solitary wave evolution, i.e. snapshots taken at different times (with equal time intervals) and plotted together. Shown in Fig .2, a solitary wave with amplitude $A = 0.2$ propagates from left to right and the wave peak reaches the leading and trailing edges of the plate approximately at $t = t_1$ and $t = t_2$, respectively. For comparison purpose, we also show in this figure evolution of the same solitary wave propagating over the same plate, which is fixed in place at $\zeta_0 = 0.4$. See [22] for the GN model on wave interaction with a submerged fixed plate.

The wave undergoes significant deformation as it approaches the oscillating plate. The wave deformations are more remarkable in the case of the oscillating plate when compared to the fixed plate. Shown in Fig.2, we also find that small waves with decreasing amplitude are reflected upwave when the solitary wave peak approaches the leading edge of the plate at $t = t_1$. It is found that amplitudes of reflected waves by an oscillating plate are significantly larger than those by a fixed plate. It is shown in the figure, compared with the fixed plate, that the speed of the main wave changes more remarkably when it is passing over the oscillating plate. We can also observe that the main wave is followed by smaller tail waves when it is passing the plate trailing edge at $t > t_2$, i.e. when the wave is propagating from shallow to deep section. We find that amplitudes of these tail waves are larger for the case of the oscillating plate than the fixed plate.

Time series of position of the oscillating and fixed plates under the solitary wave are presented in Fig. 3. Shown in the figure, the oscillating plate experiences the largest oscillation when the main wave is approaching the leading edge and when it is passing over the plate at $t_1 \leq t \leq t_2$. We can also observe smaller oscillation amplitudes due to interaction between the plate and reflected small waves when $t_2 \leq t \leq t_3$, and the oscillations are not remarkable after the main wave is far away from the plate i.e. at $t > t_3$.

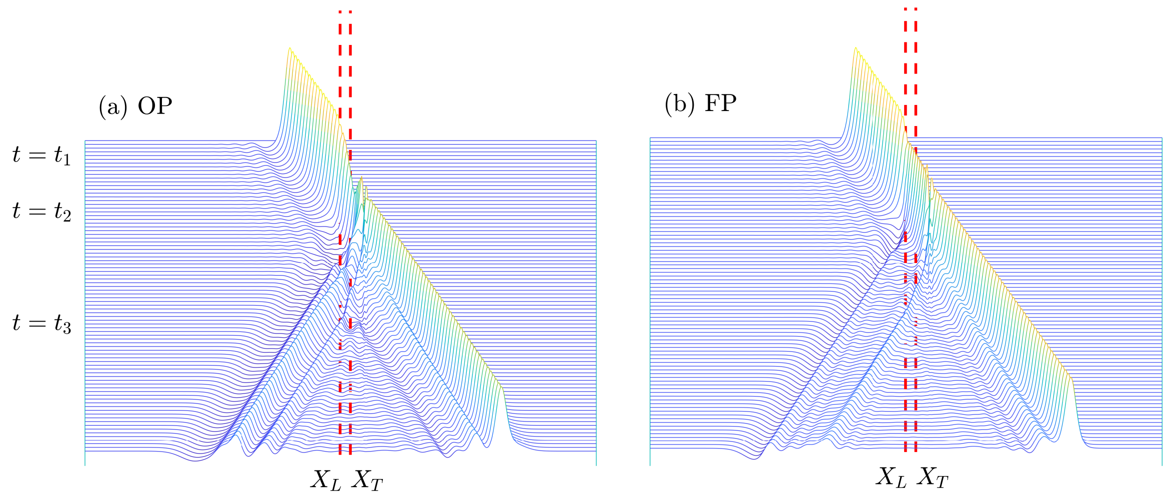

Fig. 2: Solitary wave evolution due to (a) the submerged oscillating plate (OP) and (b) the submerged fixed plate (FP) for wave amplitude $A = 0.2$, $L_P = 10$, $\zeta_0 = 0.4$, $m = 4$ and $k = 12$. The red dashed lines are the location of the leading (X_L) and trailing (X_T) edges of the plate.

4.2 Comparisons of Time Series

In this section, we compare time series of surface elevation of cnoidal waves propagating over the submerged oscillating plate calculated by the GN model with the available data, including laboratory experiments, and the Navier-Stokes (NS) and linear models of [19]. Figure 4 shows the time series of surface elevation, obtained by the GN, and the available data of laboratory measurements, and the NS and linear models, recorded at $x_1 = X_L - 2$ upwave from the leading edge of the plate, and $x_1 = X_T + 2$ downwave from the trailing edge, for two wave heights, $H = 0.067$ and $H = 0.133$. The length and mass of the plate are $L_P = 1$ and $m = 0.016$, respectively. The nonlinear GN model shows very good agreement with the laboratory experiments, indicating that nonlinearity is important in wave interaction with a submerged freely oscillating plate, see [19] for further discussion about the agreement of the GN model with the available data. The NS and linear approaches predict slightly smaller upwave amplitude than that of the GN model. The GN and NS models show closer agreement downwave of the plate.

Next, time series of the surface elevation and plate oscillations, calculated by the GN is compared with the NS model of [19], shown in Fig. 5 for $\zeta_0 = 0.4$, and $k = 3$, Fig. 6 for $\zeta_0 = 0.6$, and $k = 3$, and Fig. 7 for $\zeta_0 = 0.4$, and $k = 15$. The length and mass of the plate are $L_P = 3$ and $m = 0.35$, respectively. The locations of gauges upwave

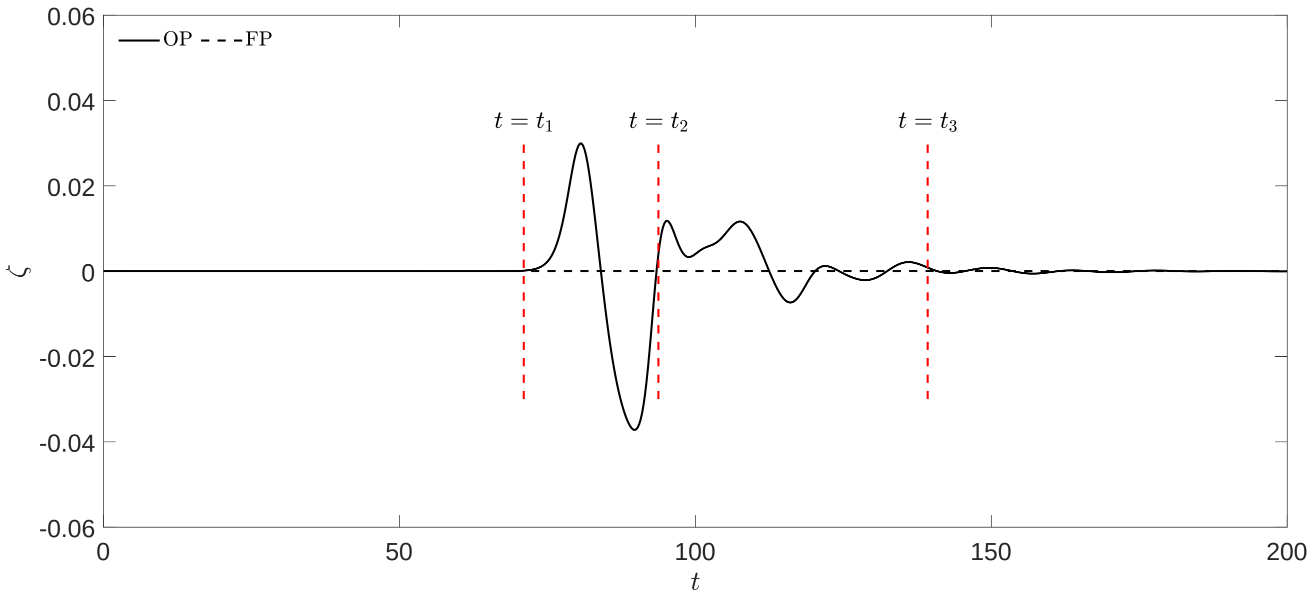

Fig. 3: Time series of oscillations of the submerged oscillating plate (OP) and the submerged fixed plate (FP) under the solitary wave, $A = 0.2$, $L_P = 10$, $\zeta_0 = 0.4$, $m = 4$ and $k = 12$.

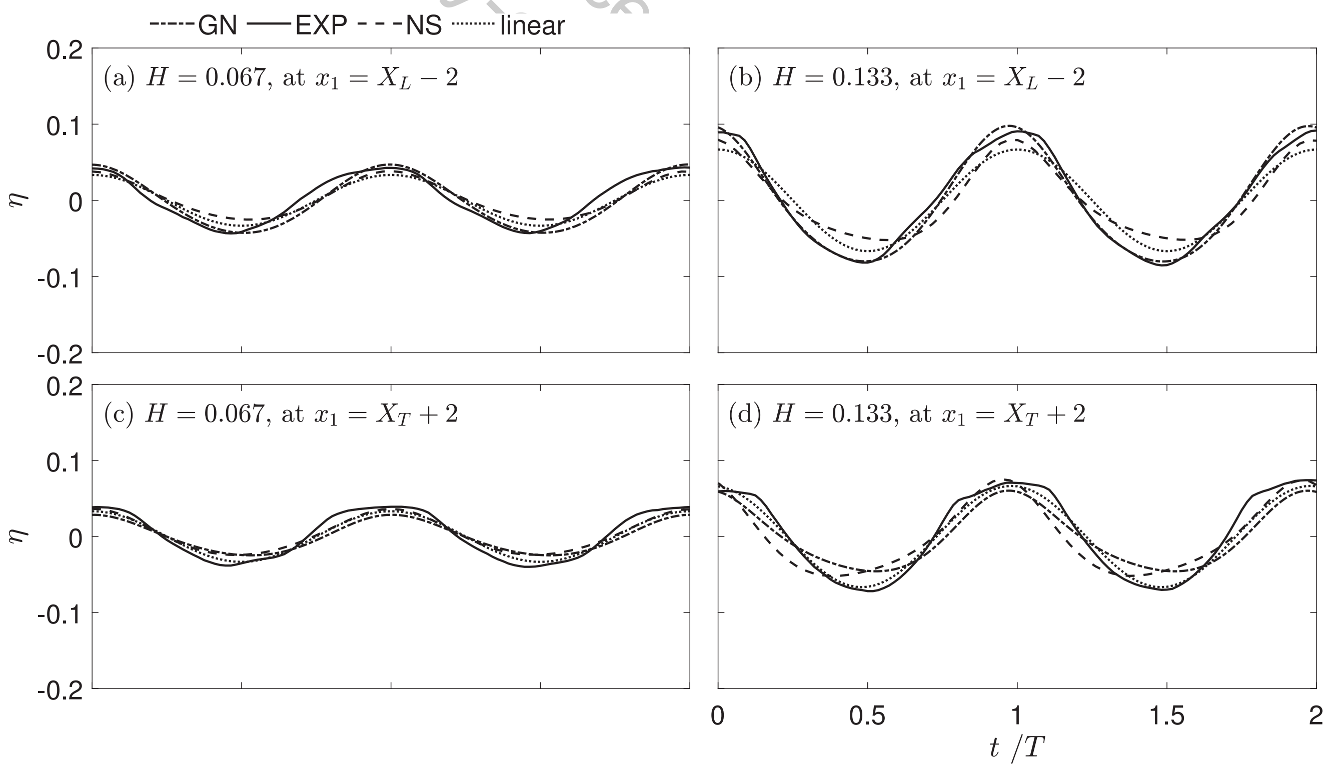

Fig. 4: Comparison of time series of surface elevation of cnoidal waves over a submerged oscillating plate, recorded upwave (a, b) and downwave (c, d) for $H = 0.067$ and $H = 0.133$ by the GN and laboratory experiments, and NS and linear models of [19]. $T = 10$, $\zeta_0 = 0.3$, and $k = 0.041$.

for GI and GII and downwave for GIII and GIV are fixed at $x_1 = X_L - 6$ and $x_1 = X_L - 3$, and $x_1 = X_T + 3$ and $x_1 = X_T + 6$, respectively, and GV is placed above the center of the plate.

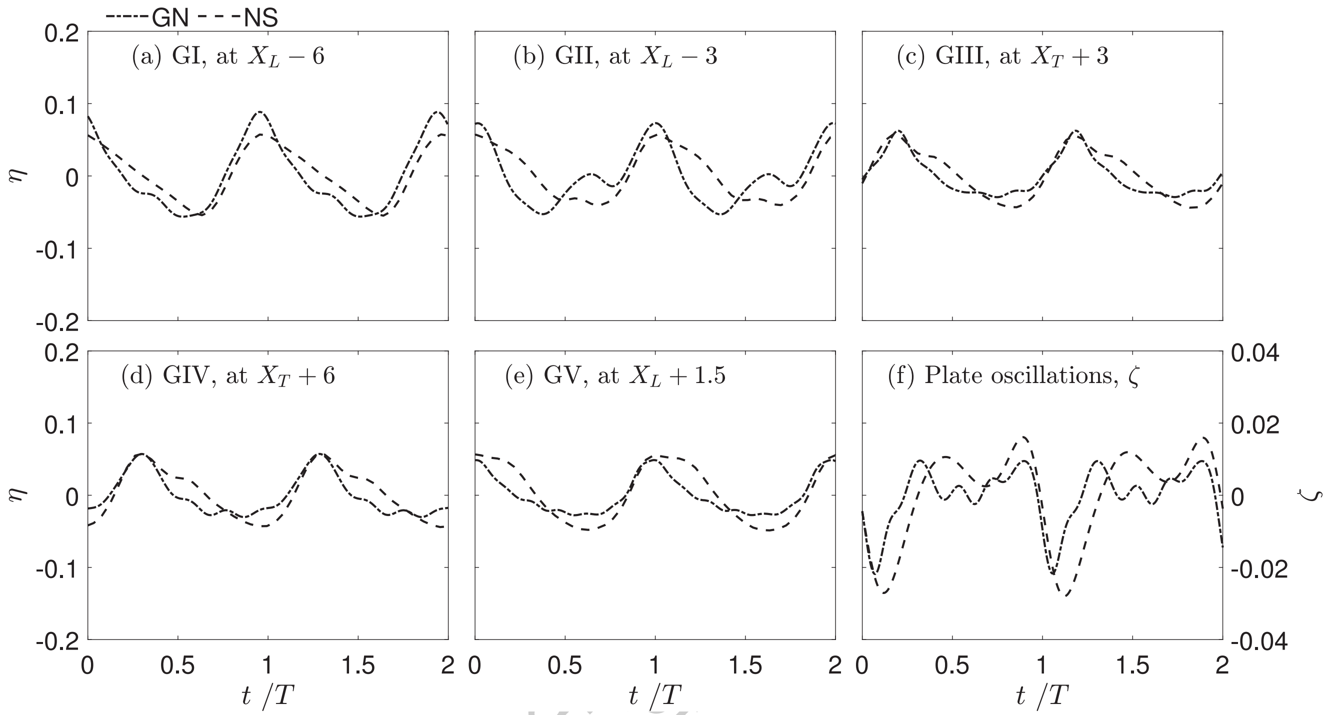

Fig. 5: Comparisons of (a-e) time series of surface elevation and (f) plate oscillations by the NS and GN models for $\zeta_0 = 0.4$ and $k = 3$. $T = 25$, $H = 0.1$.

Shown in Figs. 5, 6 and 7, the GN model predicts the peak of the surface elevation slightly larger in GI, upwave from the leading edge. In all other gauges, results of the GN model are in close agreement with the NS model particularly at the downwave gauges. Plate oscillations, ζ, obtained by the two models are in good agreement in all cases.

4.3 Cnoidal Wave Scattering

In this subsection, wave reflection and transmission coefficients are calculated and their nonlinear components up to the third-order harmonics are considered. All results presented in this section (and the remaining parts of this manuscript) are for cnoidal waves. Results are obtained by use of the GN model, and presented and discussed for a range of variables. Wave Gauges GI, GII, GIII and GIV, used in this section, are placed upwave and downwave as shown in Fig. 1, and their locations are determined depending on the wavelength (λ) and given in Table 1 for the various conditions considered here.

A wide range of parameters, including wavelength, wave height, plate length, initial submergence depth of the plate, spring stiffness and damping coefficients, are considered to investigate their effect on the wave scattering, presented by $C_R^{(n)}$ and $C_T^{(n)}$. Values of these variables are given in Table 2. The length and mass of the oscillating plate are $L_P = 2$ and $m = 0.2$, respectively, and are constant in all cases in this section. $C_d = 0.0$, in this section, unless otherwise stated.

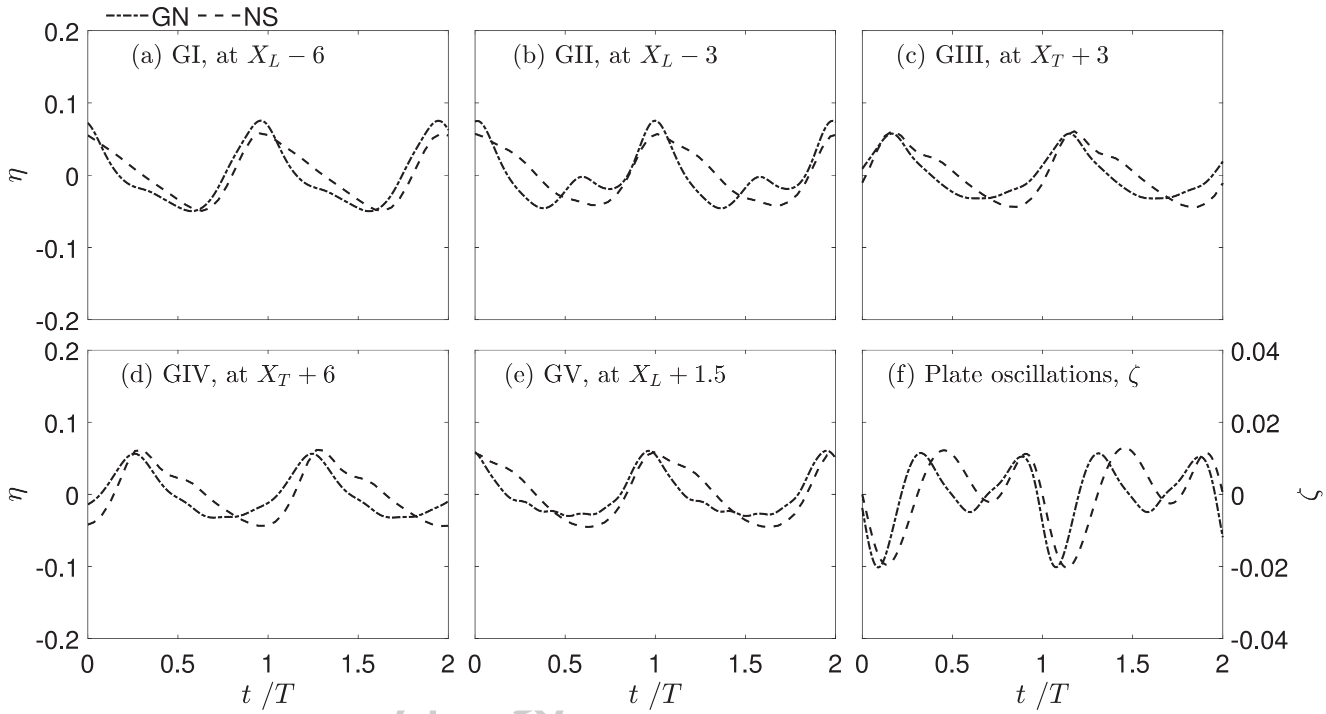

Fig. 6: Comparisons of (a-e) time series of surface elevation and (f) plate oscillations by the NS and GN models for $\zeta_0 = 0.6$ and $k = 3$. $T = 25$, $H = 0.1$.

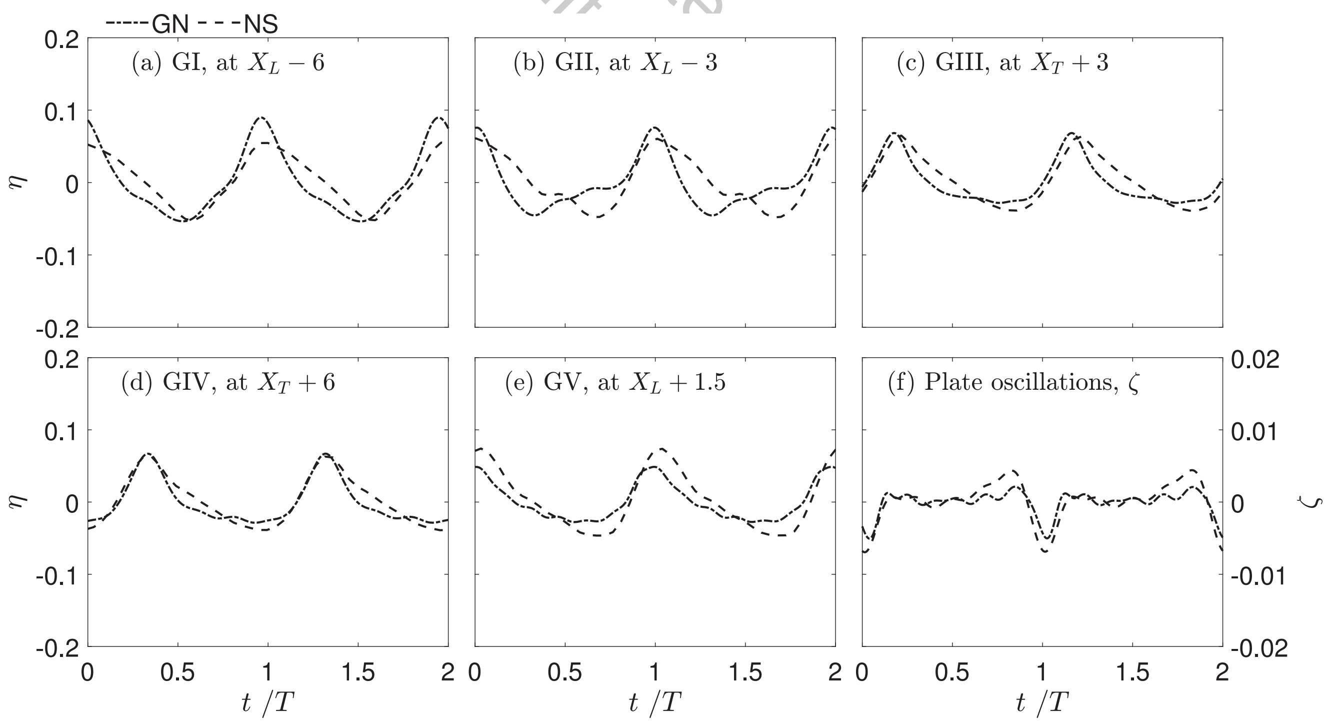

Fig. 7: Comparisons of (a-e) time series of surface elevation and (f) plate oscillations by the NS and GN models for $\zeta_0 = 0.4$ and $k = 15$. $T = 25$, $H = 0.1$.

Table 1: Wave gauge locations with variation of wavelength.

λ	GI	GII	GIII	GIV
6	$X_L - 10$	$X_L - 7.7$	$X_T + 7.7$	$X_T + 10$
8	$X_L - 10$	$X_L - 7.7$	$X_T + 7.7$	$X_T + 10$
10	$X_L - 10$	$X_L - 7.7$	$X_T + 7.7$	$X_T + 10$
12	$X_L - 10$	$X_L - 7.7$	$X_T + 7.7$	$X_T + 10$
16	$X_L - 10$	$X_L - 5.4$	$X_T + 5.4$	$X_T + 10$
20	$X_L - 10$	$X_L - 5.4$	$X_T + 5.4$	$X_T + 10$
24	$X_L - 10$	$X_L - 5.4$	$X_T + 5.4$	$X_T + 10$

Table 2: Values of variables considered in this study.

Variables	Values
Wavelength, λ	6, 8, 10, 12, 16, 20, 24
Wave height, H	0.1, 0.15, 0.2, 0.25, 0.3, 0.35, 0.4
Plate length, L_P	1, 2, 3, 4
Initial submergence depth, ζ_0	0.2, 0.3, 0.4, 0.5, 0.6
Spring stiffness, k	0.3, 0.6, 1, 2, 3, 4, 6, 8, 10
Damping coefficient, C_d	0.0, 1.0, 5.0

4.3.1 Effect of Wavelength

Figure 8 shows the variation of $C_R^{(n)}$ and $C_T^{(n)}$ with λ/L_P for different initial submergence depths, $\zeta_0 = 0.2$, 0.4 and 0.6. Shown in Fig. 8, $C_R^{(n)}$ and $C_T^{(n)}$vary nonlinearly with λ/L_P. The nonlinear components, $C_R^{(2)}$ and $C_T^{(2)}$, and $C_R^{(3)}$ and $C_T^{(3)}$, play more remarkable roles for longer waves, at $\lambda/L_P \geq 5$, in most cases.

Shown in Fig. 8, the smallest $C_R^{(1)}$ value is observed at the largest wavelength ($\lambda/L_P = 12$), for larger initial submergence depths ($\zeta_0 = 0.4$ and 0.6). This is because in the presence of long waves, the plate size compared to the size of the wave is small, hence the plate has smaller effect on the wave. Also, the wave-induced oscillations are less remarkable when the plate is submerged farther from the free surface. Peaks of $C_R^{(2)}$ and $C_R^{(3)}$ occur at $\lambda/L_P = 8$ for $\zeta_0 = 0.4$ and 0.6. The peak values of $C_R^{(2)}$ and $C_R^{(3)}$ at $\zeta_0 = 0.2$ are larger than that at $\zeta_0 = 0.4$ and 0.6, which shows that nonlinear effects play a more important role when the plate oscillates closer to the free surface, and this is of course not surprising. $C_T^{(1)}$ is nearly constant with increasing λ/L_P, while $C_T^{(2)}$ and $C_T^{(3)}$ are increasing in most cases.

4.3.2 Effect of Wave Height

Figure 9 shows variation of $C_R^{(n)}$ and $C_T^{(n)}$ with various wave heights for $C_d = 0.0$, 1.0 and 5.0. Shown in Fig. 9, $C_R^{(n)}$ and $C_T^{(n)}$ vary nonlinearly with wave height. Also, the damping coefficients hardly affect the wave reflection and transmission coefficients.

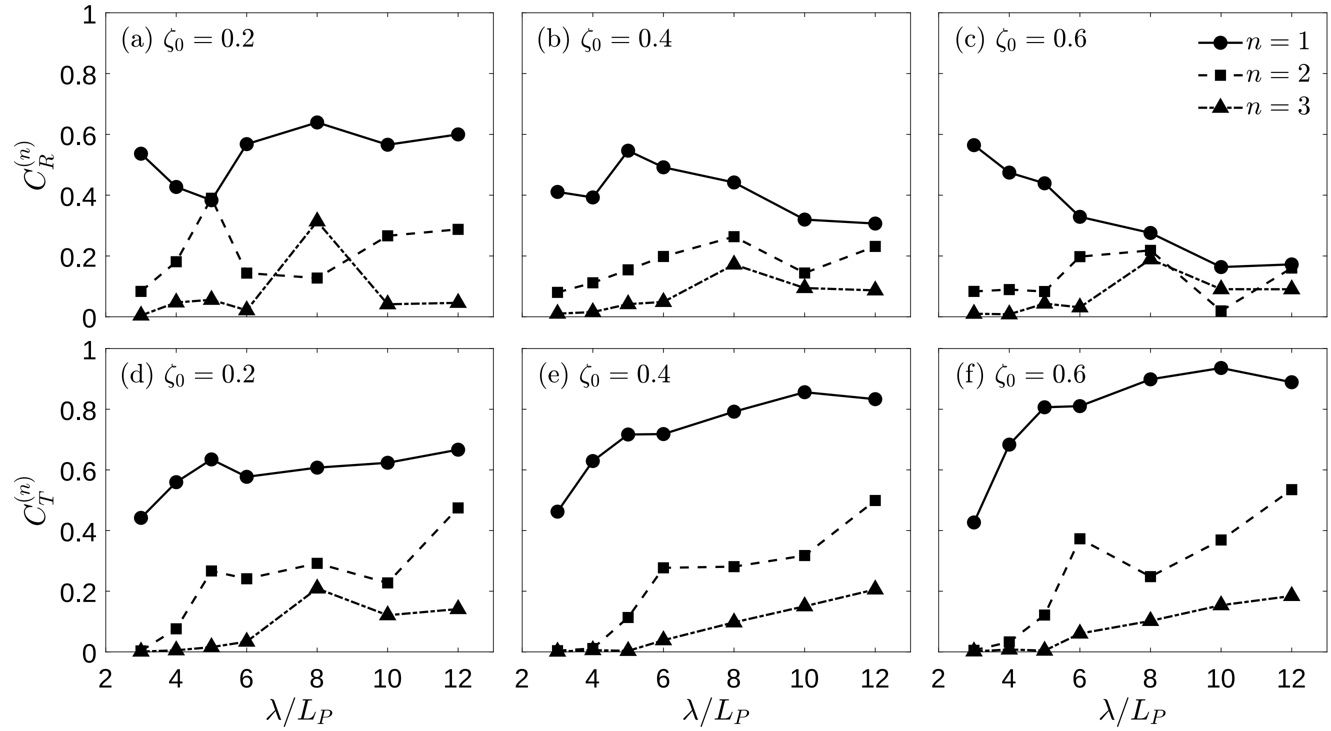

Fig. 8: Variation of (a)-(c) wave reflection and (d)-(f) transmission coefficients with λ/L_P for $\zeta_0 = 0.2$, 0.4 and 0.6, and $H = 0.2$ and $k = 3$ are constant.

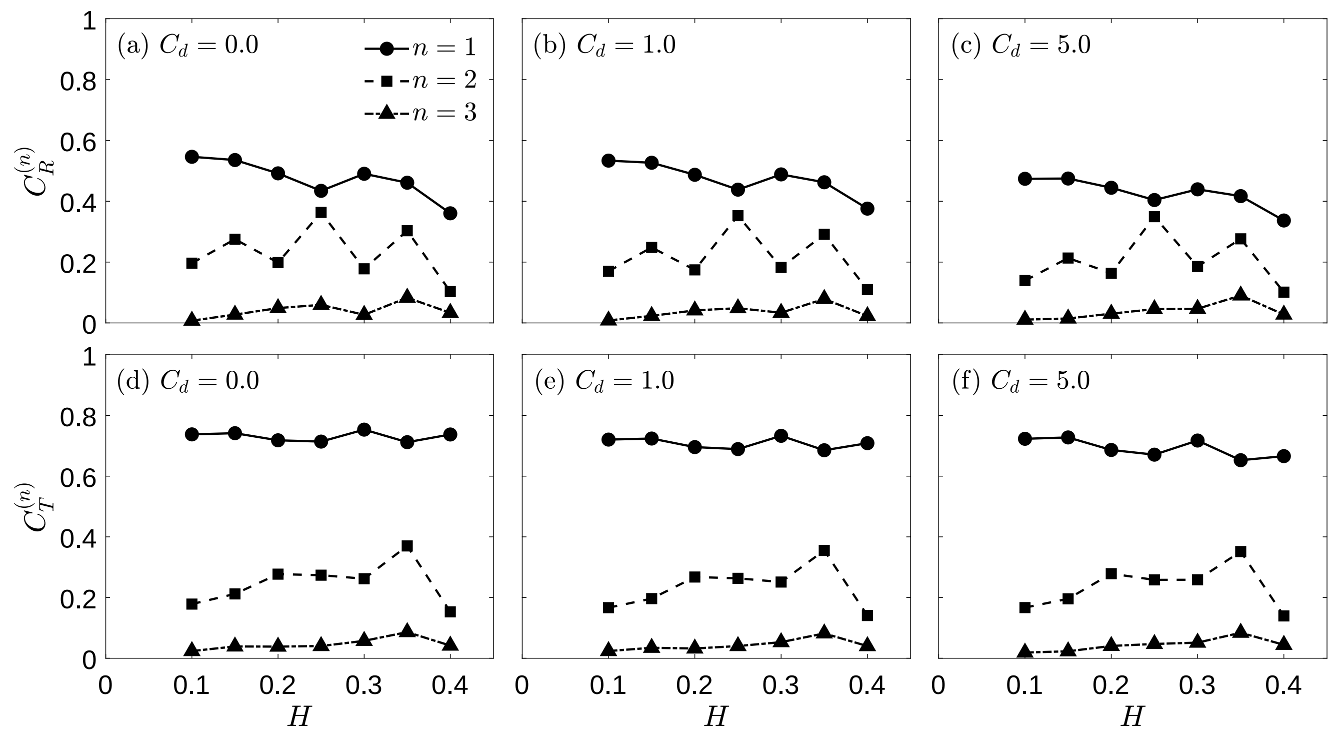

Fig. 9: Variation of (a)-(c) wave reflection and (d)-(f) transmission coefficients with wave height H for $C_d = 0.0$, 1.0 and 5.0, and $\lambda = 12$, $\zeta_0 = 0.4$ and $k = 3$ are constant.

Shown in Fig. 9, $C_R^{(1)}$ and $C_R^{(2)}$ are smallest at $H = 0.4$ for all cases because of the largest value for nonlinearity. $C_R^{(1)}$ generally decreases with increasing wave height while $C_R^{(2)}$ is oscillatory from $H = 0.1$ to $H = 0.4$, and its maximum value occur at an intermediate wave height, $H = 0.25$. The third-order components, $C_R^{(3)}$ and $C_T^{(3)}$, are remarkably smaller in all wave heights. Values of $C_T^{(1)}$ show less variation with wave height (H), and roughly equals to 0.7 in nearly all cases. $C_T^{(2)}$ reaches a maximum value at a relatively larger wave height, $H = 0.35$, but it becomes much smaller with an increase in wave height.

4.3.3 Effect of Plate Length

Figure 10 shows the variation of $C_R^{(n)}$ and $C_T^{(n)}$ with various plate lengths for $\lambda = 6$, $\lambda = 12$ and $\lambda = 24$. The length of the plate, as considered here, is between $Lp = 1$ and $Lp = 4$, with an interval of 1. The plate density is invariant and thus its corresponding mass is between $m = 0.1$ and $m = 0.4$, with an interval of 0.1.

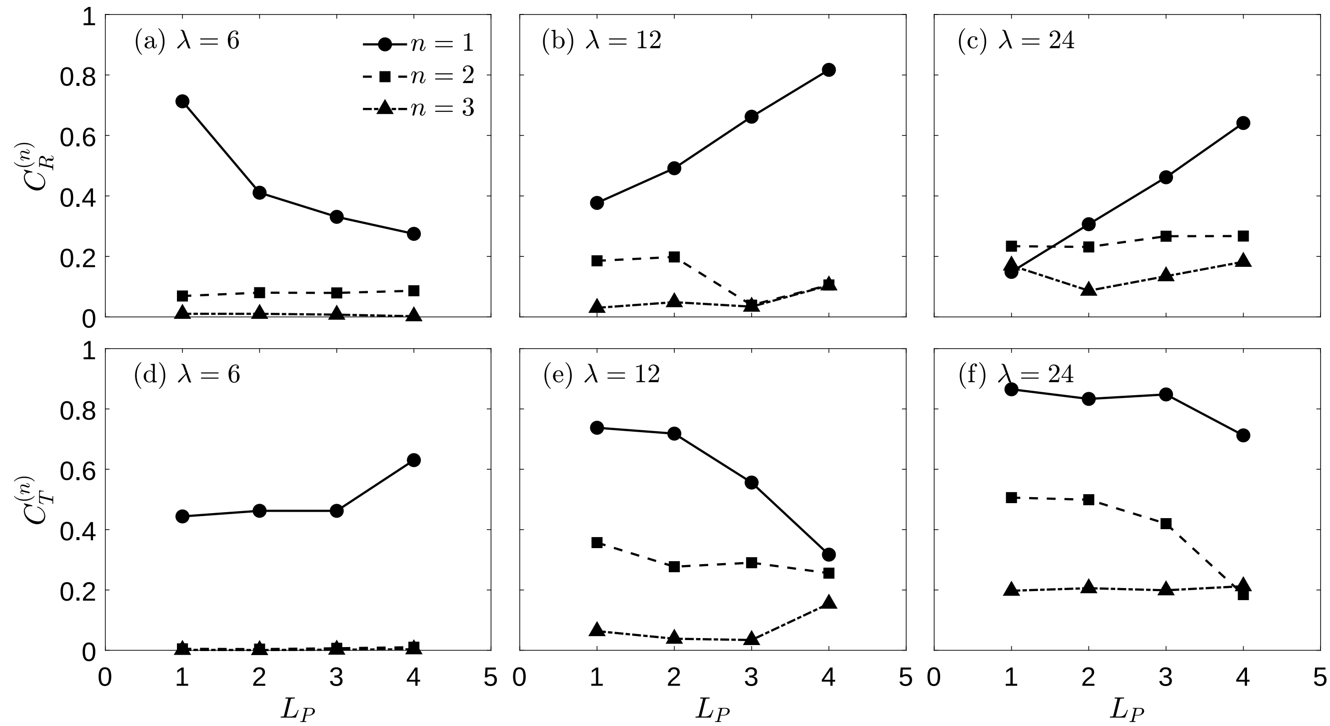

Fig. 10: Variation of (a)-(c) wave reflection and (d)-(f) transmission coefficients with plate length L_P for $\lambda = 6$, 12 and 24, and $H = 0.2$ and $\zeta_0 = 0.4$ are constant.

As shown in Fig. 10, we find that wave reflection and transmission vary nonlinearly with plate length. The second-order and third-order harmonics rarely contribute to wave reflection and transmission for $\lambda = 6$. In this figure, $C_R^{(1)}$ is reversely changed with plate length for $\lambda = 6$ while $C_R^{(1)}$ is almost positively proportional with L_P for $\lambda = 12$ and $\lambda = 24$. This is mainly because the bottom pressure of the oscillating plate are distributed in a parabolic form. Wave forces acting on the plate vary nonlinearly with increasing plate lengths and thus plate oscillations are not identical even for the same λ/L_P, but a different plate length. Note that plate lengths are nondimensionalized by the fixed water depth, h.

4.3.4 Oscillating vs Fixed Submerged Plate

In this section, we investigate differences in wave scattering by a horizontal submerged oscillating plate and an equivalent horizontal submerged fixed plate. Identical wave-plate conditions are used for the fixed and oscillating submerged plates to allow for a direct comparison of the results. The only difference is that we use the model discussed here for the oscillating plate, while the model of [22] is used for the fixed plate, which utilizes the Level I GN theory. See [4] for a parametric study of wave scattering by a fixed, submerged horizontal plate.

Figure 11 shows that surface elevation time series recorded in Gauges GI and GII upwave, Gauges GIII and GIV downwave, and Gauge GV above the center of the oscillating plate are compared to that of the fixed plate. Shown in Fig. 11, wave amplitudes scattered by the oscillating plate are slightly larger in Gauge GI while the wave heights scattered by the oscillating plate are smaller in other gauges, particularly in Gauges GII and GV.

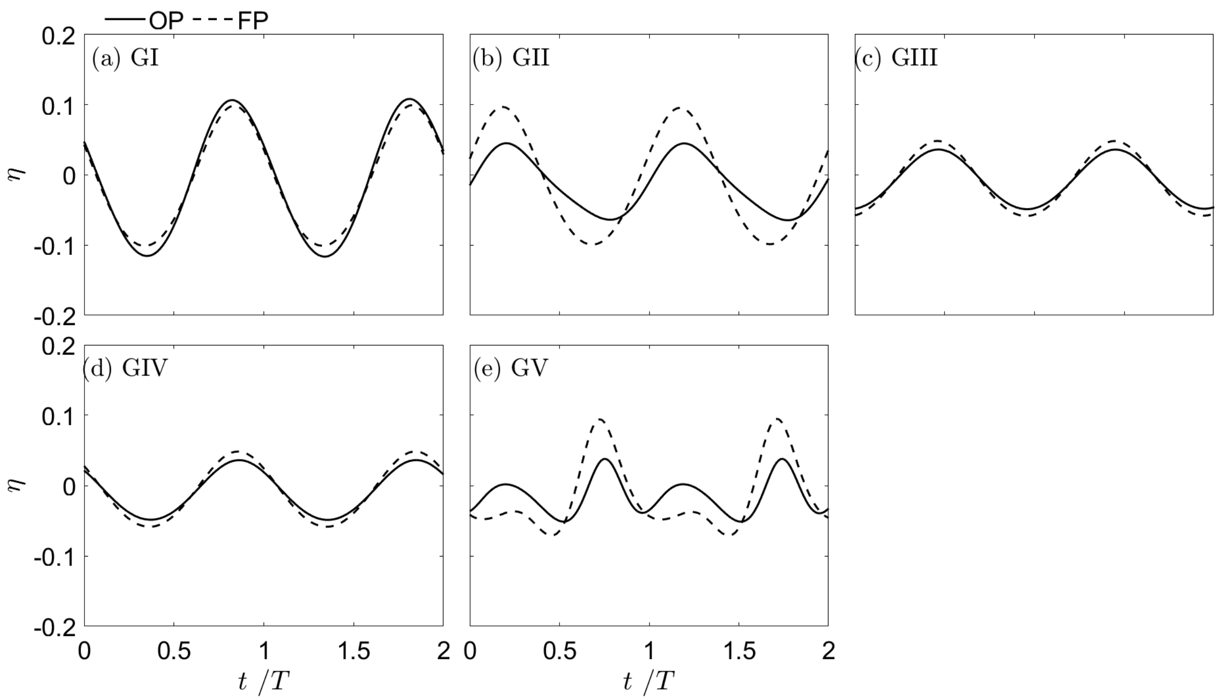

Fig. 11: Comparisons of time series of surface elevation for (a, b) Gauges GI and GII upwave, (c, d) GIII and GIV downwave, and (d) GV above center of the plate, scattered by the oscillating plates (OP) and the fixed plates (FP). $\lambda = 6$, $H = 0.2$, $\zeta_0 = 0.5$, and $k = 3$.

Figure 12 illustrates variation of $C_R^{(n)}$ and $C_T^{(n)}$, of the oscillating plate and fixed plate with ζ_0 for three wavelengths $\lambda = 6$, 12 and 24. In Fig. 12, we can observe remarkable differences between the oscillating plate and fixed plate for shorter wavelength ($\lambda = 6$). However, $C_R^{(n)}$ and $C_T^{(n)}$, of the oscillating plate are much closer to the fixed plate for the longer wavelength ($\lambda = 24$). This is because pressure differences above and below the oscillating plate are not remarkable for long water waves, and thus the plate oscillations are limited, see [19].

Variation of $C_R^{(n)}$ and $C_T^{(n)}$ of the oscillating plate with various spring stiffness for $\lambda = 6$, $\lambda = 12$ and $\lambda = 24$ are shown in Fig. 13. Similar to that in Fig. 8, nonlinearity has more significant effect on longer waves for different spring stiffness. The oscillating plates with a weaker spring attached to, i.e. $k \leq 1$, allow larger oscillations, and this causes larger wave reflection. Also results of $C_R^{(n)}$ and $C_T^{(n)}$ by the same submerged fixed plate are presented and compared in the figure. We observe that wave reflection and transmission coefficients of the oscillating plate

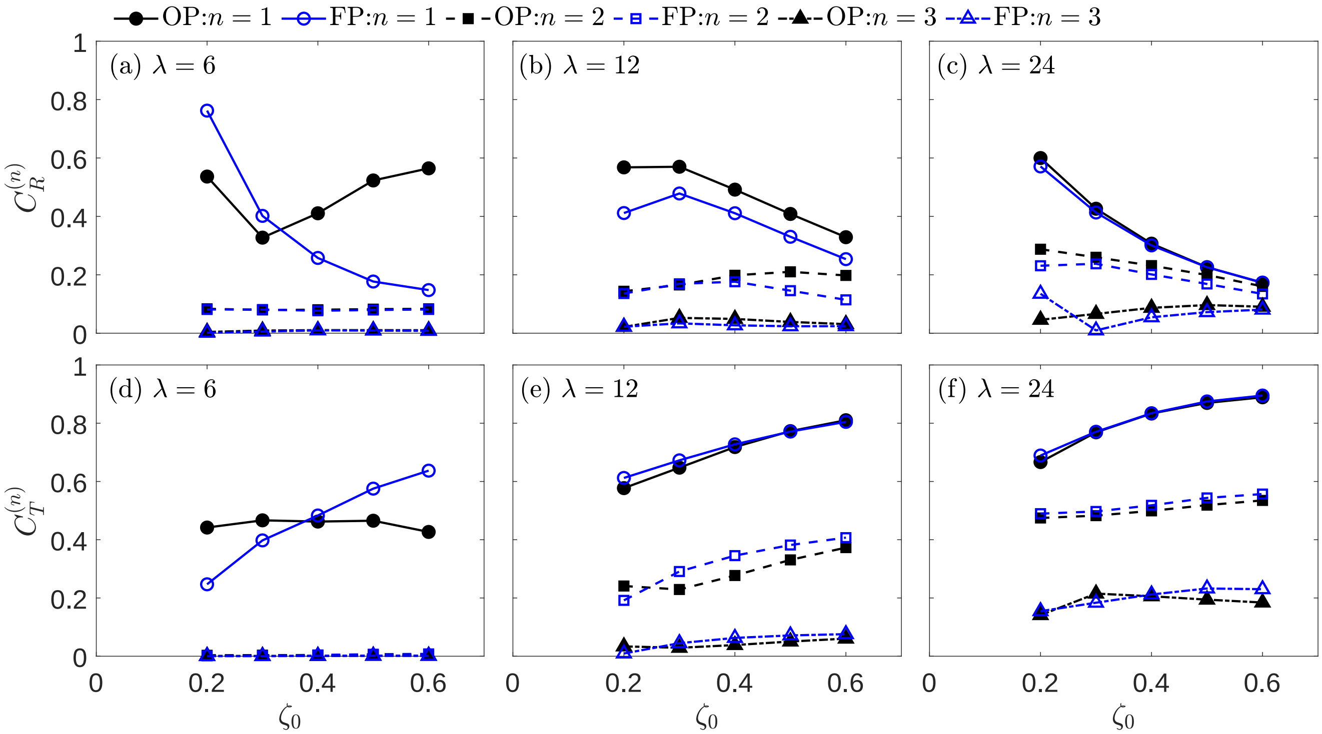

Fig. 12: Variation of (a)-(c) wave reflection and (d)-(f) transmission coefficients of oscillating plates (OP) vs fixed plates (FP) with ζ_0 for $\lambda = 6$, 12 and 24, and $H = 0.2$ and $k = 3$ are constant.

tend to be invariant with increasing spring stiffness. We can also observe that wave reflection and transmission scattered by an oscillating plate connected to a relatively strong spring, are much closer to those by a fixed plate, i.e. the wave field scattered by an oscillating plate with a strong spring is similar to that by a equivalent fixed plate.

5 CONCLUDING REMARKS

In this study, a model based on the nonlinear Level I Green-Naghdi equations for wave propagation over submerged oscillating plates is developed. Attention is confined to wave scattering by an oscillating plate in shallow water. Wave reflection and transmission coefficients, $C_R^{(n)}$ and $C_T^{(n)}$, are determined to evaluate the reflected and transmitted waves, respectively. To investigate the contributions of nonlinear components to scattered waves, the first three harmonics are considered in this study.

Time series of surface elevation of the model are compared with the laboratory experiments, the NS and linear models of [19]. Good agreement is observed between the GN results and experimental data and the other two numerical results.

Variations of $C_R^{(n)}$ and $C_T^{(n)}$ with various parameters, including wavelength, wave height, plate length, initial submergence depth of the plate, spring stiffness and damping coefficients, are investigated as well in this study. Overall nonlinear harmonics play an important role to determine wave scattering by the oscillating plate in shallow water. $C_R^{(2)}$ and $C_T^{(2)}$, are remarkable in most cases while $C_R^{(3)}$ and $C_T^{(3)}$, are less significant.

In this study, a wide range of parameters are considered to investigate their effect on wave scattering by a submerged oscillating plate. It is found that $C_R^{(n)}$ and $C_T^{(n)}$ vary nonlinearly with λ/L_P. Nonlinear harmonic components play a more remarkable role on the wave scattering for longer waves. Initial submergence depth of the oscillating plate has more significant influence on the first harmonic, $C_R^{(1)}$ and $C_T^{(1)}$, than that of the higher-order

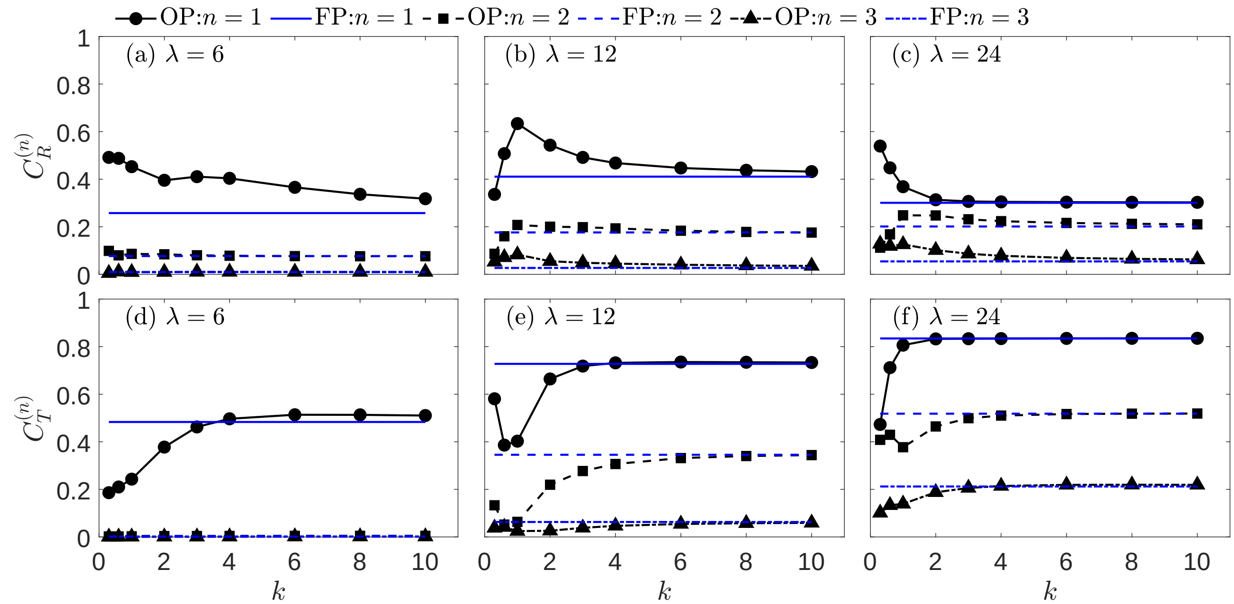

Fig. 13: Variation of (a)-(c) wave reflection and (d)-(f) transmission coefficients of oscillating plates (OP) vs fixed plates (FP) with spring stiffness k for $\lambda = 6$, 12 and 24, and $H = 0.2$ and $\zeta_0 = 0.4$ are constant.

components. The effect of wave height on $C_T^{(n)}$ is less than that on $C_R^{(n)}$. The damping coefficients show small effect on $C_R^{(n)}$ and $C_T^{(n)}$ for the cases considered in this study. Plate lengths nonlinearly affect the plate oscillations, and wave reflection and transmission coefficients are not identical for the same λ/L_P, but a different plate length. Springs, attached to the plate, dominate the performance of wave scattering. It is also found that wave scattering is hardly altered with relatively stronger springs, i.e., $C_R^{(n)}$ and $C_T^{(n)}$ of the oscillating plate are almost invariant, like an equivalent fixed plate.

Wave scattering by an oscillating plate are calculated by use of the GN model, and compared with that of a fixed plate. We find that differences of wave scattering by the oscillating and fixed plates are more remarkable for shorter waves. Overall, it is observed that an oscillating submerged plate can have remarkable effect on the wave field. In almost all cases considered here, the presence of the oscillating plate increases the nonlinearity of the flow field.

References

[1] Liu, P. L.-F., and Iskandarani, M., 1991. "Scattering of short-wave groups by submerged horizontal plate". *Journal of Waterway, Port, Coastal, and Ocean Engineering,* ***117***(3), pp. 235–246.

[2] Carter, R. W., Ertekin, R. C., and Lin, P., 2006. "On the reverse flow beneath a submerged plate due to wave action". In International Conference on Offshore Mechanics and Arctic Engineering, OMAE2006, June 4-9, Hamburg, Germany, pp. 92623(1–8).

[3] Brossard, J., Perret, G., Blonce, L., and Diedhiou, A., 2009. "Higher harmonics induced by a submerged horizontal plate and a submerged rectangular step in a wave flume". *Coastal Engineering,* ***56***(1), pp. 11–22.

[4] Hayatdavoodi, M., Ertekin, R. C., and Valentine, B. D., 2017. "Solitary and cnoidal wave scattering by a submerged horizontal plate in shallow water". *AIP Advances,* ***7***, pp. 065212–29.

[5] Huang, L., and Li, Y., 2022. "Design of the submerged horizontal plate breakwater using a fully coupled hydroelastic approach". *Computer-Aided Civil and Infrastructure Engineering,* ***37***(7), pp. 915–932.

[6] Zheng, S., Liang, H., Michele, S., and Greaves, D., 2023. "Water wave interaction with an array of sub-

merged circular plates: Hankel transform approach". *Physical Review Fluids*, ***8***(1), p. 014803.

[7] Liu, C. R., Huang, Z. H., and Chen, W. P., 2017. "A numerical study of a submerged horizontal heaving plate as a breakwater". *Journal of Coastal Research*, ***33***(4), pp. 917–930.

[8] He, M., Xu, W., Gao, X., and Ren, B., 2018. "SPH simulation of wave scattering by a heaving submerged horizontal plate". *International Journal of Ocean and Coastal Engineering*, ***1***(02), p. 1840004.

[9] Fu, D., Zhao, X. Z., Wang, S., and Yan, D. M., 2021. "Numerical study on the wave dissipating performance of a submerged heaving plate breakwater". *Ocean Engineering*, ***219***, p. 108310.

[10] Mendoza, E., Silva, R., Zanuttigh, B., Angelelli, E., Andersen, T. L., Martinelli, L., Nørgaard, J. Q. H., and Ruol, P., 2014. "Beach response to wave energy converter farms acting as coastal defence". *Coastal Engineering*, ***87***, pp. 97–111.

[11] Borgarino, B., Babarit, A., and Ferrant, P., 2012. "Impact of wave interactions effects on energy absorption in large arrays of wave energy converters". *Ocean Engineering*, ***41***, pp. 79–88.

[12] Carter, R. W., and Ertekin, R. C., 2014. "Focusing of wave-induced flow through a submerged disk with a tubular opening". *Applied Ocean Research*, ***47***, pp. 110–124.

[13] Newman, J. N., 2015. "Amplification of waves by submerged plates". In 30th international workshop on water waves and floating bodies (IWWWFB), Bristol, UK, pp. 153–156.

[14] Zheng, S., Meylan, M., Greaves, D., and Iglesias, G., 2020. "Water-wave interaction with submerged porous elastic disks". *Physics of Fluids*, ***32***(4), p. 047106.

[15] Liang, H., Zheng, S., Shao, Y., Chua, K. H., Choo, Y. S., and Greaves, D., 2021. "Water wave scattering by impermeable and perforated plates". *Physics of Fluids*, ***33***(7), p. 077111.

[16] Patarapanich, M., 1984. "Maximum and zero reflection from submerged plate". *Journal of Waterway, Port, Coastal, and Ocean Engineering*, ***110***(2), pp. 171–181.

[17] Dick, T. M., and Brebner, A., 1968. "Solid and permeable submerged breakwaters". *Coastal Engineering*, pp. 1141–1158.

[18] Hayatdavoodi, M., Wagner, J. J., Wagner, J. R., and Ertekin, R. C., 2016. "Vertical oscillation of a horizontal submerged plate". In 31st International Workshop on Water Waves and Floating Bodies (IWWWFB), April 3-6, Plymouth, Michigan, USA.

[19] Hayatdavoodi, M., Chen, Y. B., Zhao, B. B., and Ertekin, R. C., 2023. "Experiments and computations of wave-induced oscillations of submerged horizontal plates". *Physics of Fluids*, ***35***(1), pp. 017121(1–28).

[20] Green, A. E., and Naghdi, P. M., 1976. "Directed fluid sheets". *Proceedings of the Royal Society of London. A. Mathematical and Physical Sciences*, ***347***(1651), pp. 447–473.

[21] Green, A. E., and Naghdi, P. M., 1976. "A derivation of equations for wave propagation in water of variable depth". *Journal of Fluid Mechanics*, ***78***(2), pp. 237–246.

[22] Hayatdavoodi, M., and Ertekin, R. C., 2015. "Wave forces on a submerged horizontal plate – part I: Theory and modelling". *Journal of Fluids and Structures*, ***54***, pp. 566–579.

[23] Webster, W. C., Duan, W. Y., and Zhao, B. B., 2011. "Green-Naghdi theory, Part A: Green-Naghdi (GN) equations for shallow water waves". *Journal of Marine Science and Application*, ***10***(3), pp. 253–258.

[24] Zhao, B. B., Duan, W. Y., and Ertekin, R. C., 2014. "Application of higher-level GN theory to some wave transformation problems". *Coastal Engineering*, ***83***, pp. 177–189.

[25] Zhao, B. B., Duan, W. Y., Ertekin, R. C., and Hayatdavoodi, M., 2015. "High-level Green-Naghdi wave models for nonlinear wave transformation in three dimensions". *Journal of Ocean Engineering and Marine Energy*, ***1***(2), pp. 121–132.

[26] Hayatdavoodi, M., and Ertekin, R. C., 2022. "Diffraction and refraction of nonlinear waves by the Green–Naghdi equations". *Journal of Offshore Mechanics and Arctic Engineering*, ***145***(2), p. 021201.

[27] Ertekin, R. C., 1984. *Soliton Generation by Moving Disturbances in Shallow Water: Theory, Computation and Experiment*. Ph.D. Dissertation, University of California, Berkeley.

[28] Hayatdavoodi, M., and Ertekin, R. C., 2015. "Nonlinear Wave Loads on a Submerged Deck by the Green-Naghdi Equations". *Journal of Offshore Mechanics and Arctic Engineering*, ***137***(1), p. 11102.

[29] Sun, X., 1991. *Some theoretical and numerical studies on two-dimensional cnoidal-wave-diffraction problems*. M.S. Thesis, University of Hawai'i at Manoa.
[30] Ertekin, R. C., and Becker, J. M., 1998. "Nonlinear Diffraction of Waves by a Submerged Shelf in Shallow Water". *Journal of Offshore Mechanics and Arctic Engineering,* ***120***(4), 11, pp. 212–220.
[31] Hayatdavoodi, M., and Ertekin, R. C., 2015. "Wave forces on a submerged horizontal plate – part II: Solitary and cnoidal waves". *Journal of Fluids and Structures,* ***54***, pp. 580–596.
[32] Naghdi, P. M., and Rubin, M. B., 1981. "On the transition to planing of a boat". *Journal of Fluid Mechanics,* ***103***, pp. 345–374.
[33] Hayatdavoodi, M., Treichel, K., and Ertekin, R. C., 2019. "Parametric study of nonlinear wave loads on submerged decks in shallow water". *Journal of Fluids and Structures,* ***86***, pp. 266–289.
[34] Grue, J., 1992. "Nonlinear water waves at a submerged obstacle or bottom topography". *Journal of Fluid Mechanics,* ***244***, pp. 455–476.
[35] Kostikov, V., Hayatdavoodi, M., and Ertekin, R. C., 2021. "Hydroelastic interaction of nonlinear waves with floating sheets". *Theoretical and Computational Fluid Dynamics,* ***35***, pp. 515–537.
[36] Chen, Y. B., Hayatdavoodi, M., Zhao, B. B., and Ertekin, R. C., 2023. "Wave attenuation by submerged oscillating plates". In International Conference on Offshore Mechanics and Arctic Engineering, OMAE2023, June 11-16, Melbourne, Australia, pp. 105070(1–10).